NUREG/CR-0589
HEDL-TME-78-102
RT

DYNAMIC ANALYSIS TO ESTABLISH NORMAL SHOCK AND VIBRATION OF RADIOACTIVE MATERIAL SHIPPING PACKAGES

Quarterly Progress Report
July - September 1978

S. R. Fields
S. J. Mech

Hanford Engineering Development Laboratory

Prepared for
U. S. Nuclear Regulatory Commission

Available from
National Technical Information Service
Springfield, Virginia 22161
Price: Printed Copy $4.50 ; Microfiche $3.00

The price of this document for requesters outside of the North American Continent can be obtained from the National Technical Information Service.

DISCLAIMER

NUREG/CR-0589
HEDL-TME 78-102
RT

DYNAMIC ANALYSIS TO ESTABLISH NORMAL SHOCK AND VIBRATION OF RADIOACTIVE MATERIAL SHIPPING PACKAGES

Quarterly Progress Report
July - September 1978

S. R. Fields
S. J. Mech

Hanford Engineering Development Laboratory
P. O. Box 1970
Richland, WA 99352

Manuscript Completed: November 1978
Date Published: March 1979

MASTER

Prepared for
Division of Safeguards, Fuel Cycle, and Environmental Research
Office of Nuclear Regulatory Research
U. S. Nuclear Regulatory Commission
Washington, D.C. 20555
Under Contract No. NRC-60-78-254

 EHB

NUREG/CR-0589
HEDL-TME 78-102
RT

DYNAMIC ANALYSIS TO ESTABLISH NORMAL SHOCK AND VIBRATION OF RADIOACTIVE MATERIAL SHIPPING PACKAGES QUARTERLY PROGRESS REPORT JULY - SEPTEMBER 1978

S. R. Fields
S. J. Mech

ABSTRACT

This report presents work performed at the Hanford Engineering Development Laboratory operated by Westinghouse Hanford Company, a subsidiary of Westinghouse Electric Corporation, for the Nuclear Regulatory Commission, under Department of Energy Contract No. EY-76-C-14-2170. It describes technical progress made during the reporting period by Westinghouse Hanford Company and supporting contractors.

CONTENTS

FIGURES

TABLES

DYNAMIC ANALYSIS TO ESTABLISH NORMAL SHOCK AND VIBRATION OF RADIOACTIVE MATERIAL SHIPPING PACKAGES

QUARTERLY PROGRESS REPORT JULY - SEPTEMBER 1978

I. SUMMARY

A. DEVELOP DYNAMIC MODEL

A new calculation sequence was developed to simulate the behavior of the coupler subsystem for the cask-rail car (hammer car) and the lead car in the group it impacts (struck car) during humping operations. This new coupler submodel simulates the hysteresis-type behavior of friction draft gears. Friction draft gears consist of springs and dampers in parallel rather than the series arrangement upon which the previous calculation sequence was based. Results from this submodel compare well with experimental results for friction draft gears in their "active" state during impact (before bottoming out and during recoil). This coupler submodel will now be incorporated into the full cask-rail car model.

Since both friction draft gears and Barber stabilized trucks utilize friction damping, i.e., where friction is proportional to the load applied, the same general approach may be used to simulate the behavior of the suspension subsystem.

B. DATA COLLECTION AND REDUCTION

Eighteen rail car impact tests were completed at Savannah River Laboratories in August 1978. These tests encompassed combinations of three rail cars, two obsolete spent fuel shipping casks, four tiedown configurations, and three types of couplers. The objective of these tests was to obtain data to validate analytical models of the cask-rail car system. These data are presently being reduced and analyzed.

High speed movies were made of the coupling action of the rail car, and of the interactions of the rail car, shipping cask and tiedown mechanism. These movies have been edited and transcribed onto a video tape. An annotated version of this tape is nearly complete.

The original Sandia FM-FM instrumentation tapes were transcribed to the wide-band format required at the Hanford Engineering Development Laboratory. Data reduction is now underway.

Some data acquisition channels failed during the tests, and some data were lost because peak amplitudes estimated for calibration purposes were either too large or too small. The full significance of the lost data will not be known until data reduction has been completed; however, it is felt that it should not seriously impair the model validation objective.

D. COLLECT PARAMETER DATA

The collection of data on key parameters for the cask-rail car dynamic model was resumed during this reporting period. A data base is being established to supply the needs of the scheduled parametric and sensitivity analysis. This data base is being structured for use with a simple manual information retrieval technique to allow rapid and thorough access to the particular data types needed, without the expense of a computerized data base management system.

II. INTRODUCTION

This study was initiated in October 1977 as stated earlier in previous quarterly progress reports. The objective of this study is to determine the extent to which the shocks and vibrations experienced by radioactive material shipping packages during normal transport conditions are influenced by, or are sensitive to, various structural parameters of the transport system (i.e., package, package supports, and vehicle). The purpose of this effort is to identify those parameters which significantly affect the normal shock and vibration environments so as to provide the basis for determining the forces transmitted to radioactive material packages. Determination of these forces will provide the input data necessary for a broad range of package-tiedown structural assessments.

This is the fourth quarterly report on this work. A work plan, consisting of seven tasks, was presented in the three earlier quarterly reports. Progress on these tasks during this reporting period will now be discussed.

III. PROGRESS TO DATE

The work plan for this study, presented as Figure 1, shows the various tasks and their relation to one another. This work plan is currently being revised to reflect an adjustment in scheduling of some of the tasks. The progress on each of the tasks during this reporting period will now be presented.

A. DEVELOP DYNAMIC MODEL

A new calculation sequence has been developed to simulate the behavior of the coupler subsystem for the cask-rail car (hammer car) and the lead car in the group it impacts (struck car) during humping operations.

Friction draft gears and suspension systems actually consist of springs and dampers in parallel rather than the series arrangement upon which the previous calculation sequence was based. Therefore, the new calculation sequence is a coupler subsystem submodel based on the spring and damper arrangement shown in Figure 2(a). Like its predecessor, the present coupler submodel determines the displacements of the springs and dampers in the draft gears during normal operating conditions and when they bottom out at their limits of travel. Results from the submodel compare well with experimental results for friction draft gears during impact. (See Figures 3 and 4.) This coupler submodel will now be incorporated into the full cask-rail car model.

The equations of motion for the simple rail car-coupler subsystem model of Figure 2 are

$$M_{RC} \frac{d^2 X_{RC}}{dt^2} = - k_T (X_{RC} - X_F) \qquad (1)$$

and

$$M_F \frac{d^2 X_F}{dt^2} = k_T (X_{RC} - X_F) \qquad (2)$$

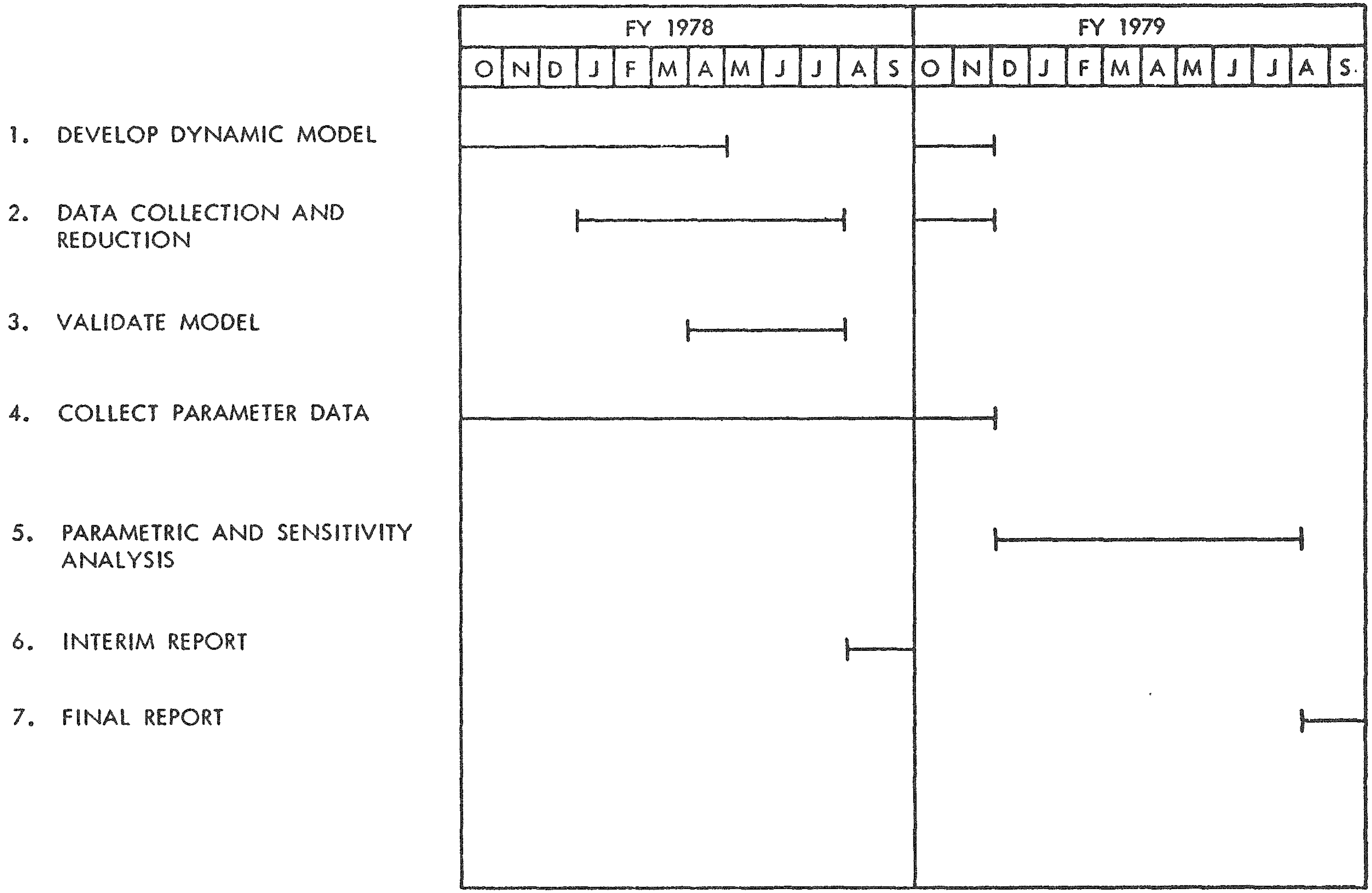

HEDL 7803-106.1

FIGURE 1. Work Plan -- Dynamic Analysis of Radioactive Material Shipping Packages.

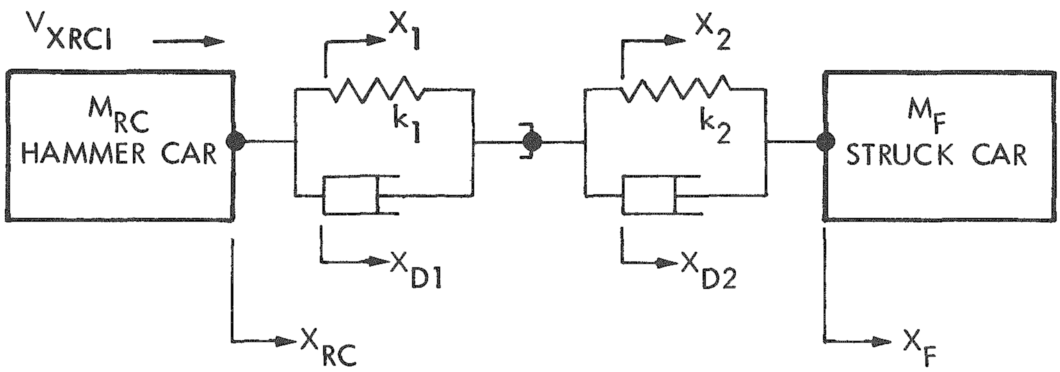

(a) COUPLER SUBSYSTEM SUBMODEL

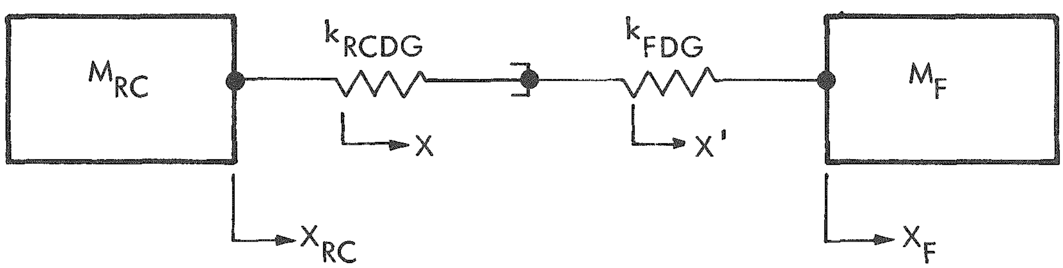

(b) COUPLER SUBSYSTEM SUBMODEL WITH EACH DRAFT GEAR REDUCED TO AN EQUIVALENT SPRING

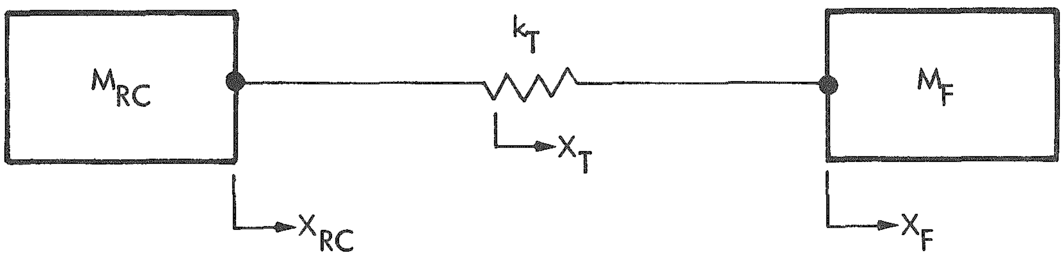

(c) COUPLER SUBSYSTEM SUBMODEL WITH BOTH DRAFT GEARS REDUCED TO ONE EQUIVALENT SPRING

HEDL 7812-133.1

FIGURE 2. Rail Car-Coupler Subsystem Model. Neg 7814254

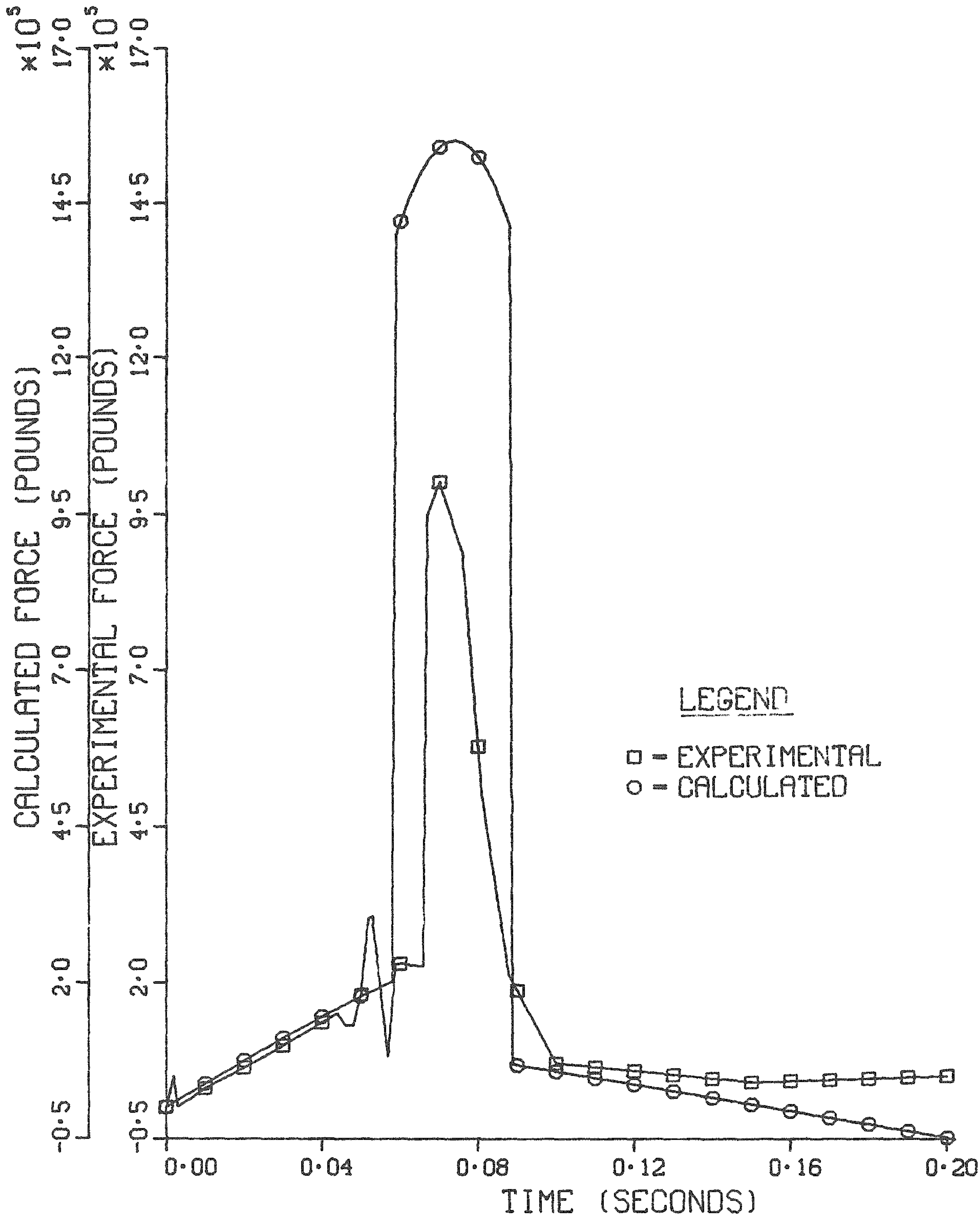

FIGURE 3. Coupler Force vs Time During Impact of Two Hopper Cars Loaded with Gravel (Spring Constant of "Solid" Draft Gears = 5 x 10^5 lb/in.).

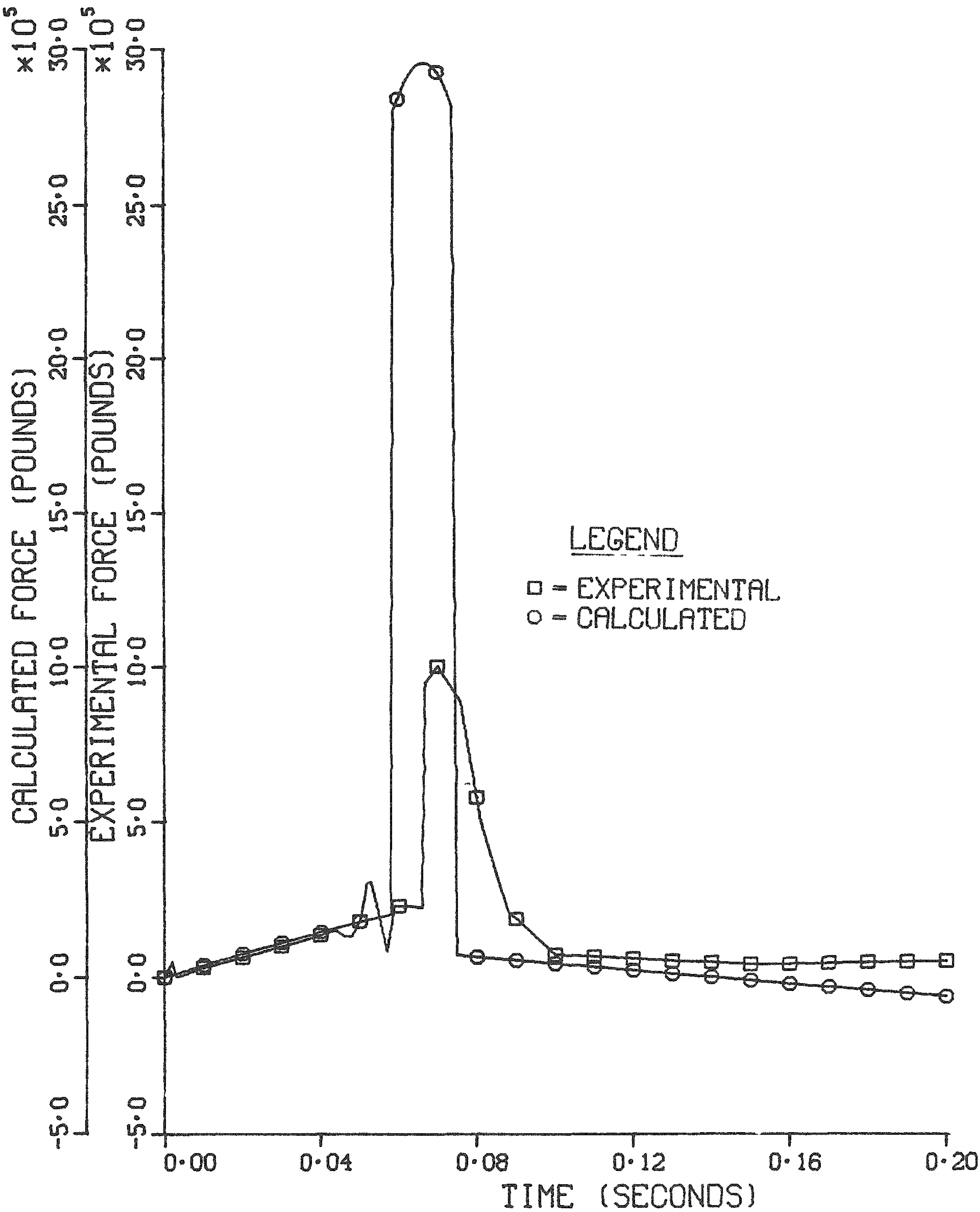

FIGURE 4. Coupler Force vs Time During Impact of Two Hopper Cars Loaded with Gravel (Spring Constant of "Solid" Draft Gears = 1 x 10^6 lb/in.).

where

X_{RC} = the displacement of the hammer car (in.)

X_F = the displacement of the struck car (in.)

M_{RC} = the mass of the hammer car, including lading

$$\left[\frac{\text{lb (force)-sec}^2}{\text{inch}}\right]$$

M_F = the mass of the struck car, including lading

$$\left[\frac{\text{lb (force)-sec}^2}{\text{inch}}\right]$$

and k_T = the total equivalent spring constant of the combined draft gears [lb (force)/in.]

An equivalent spring representing the draft gears separating the cars is obtained by combining the spring and damper of each draft gear into a single equivalent spring [Figure 2(b)] and then reducing these series-connected springs to a single spring [Figure 2(c)].

When a force is applied to a parallel arrangement of a spring and damper, such as that representing the draft gear on the hammer car in Figure 2(a), the forces and displacements are defined by

$$F_{T1} = F_1 + F_{D1} \tag{3}$$

and

$$X = X_1 = X_{D1} \tag{4}$$

respectively, where

F_{T1} = the total force applied to the draft gear on the hammer car [lb (force)]

F_1 = the force causing displacement of the spring [lb (force)]

F_{D1} = the force causing displacement of the damper [lb (force)]

X = the total travel or displacement of the draft gear on the hammer car (in.)

X_1 = the displacement of the spring (in.)

and X_{1D} = the displacement of the damper (in.)

The force on the spring is

$$F_1 = k_1 X_1 \tag{5}$$

or, since $X = X_1$

$$F_1 = k_1 X \tag{6}$$

where

k_1 = the spring constant of the spring in the hammer car draft gear [lb (force)/in.]

According to Roggeveen,[1] in a friction draft gear the friction force is caused by the spring force and is therefore proportional to it. With this in mind, the friction force or force on the damper was defined as

$$F_{D1} = \mu_D F_1 \text{ sgn } (\dot{X}) \tag{7}$$

where

μ_D = a multiplying factor corresponding to a coefficient of friction and $\mathrm{sgn}(\dot{X})$ = the signum function or sign function.

The signum function is defined as

$$\mathrm{sgn}(\dot{X}) = \begin{cases} +1 \ , & \dot{X} > 0 \\ 0 \ , & \dot{X} = 0 \\ -1 \ , & \dot{X} < 0 \end{cases} \tag{8}$$

where

$\dot{X}$ = the total relative velocity of displacement or travel of the draft gear (in./sec)

Equation (7) implies that frictional damping in the draft gear is due to the sliding of two surfaces with a friction coefficient of μ_D, pressed together by the spring force F_1. Equation (3), which defines the total force applied to the draft gear, may now be written as

$$F_{T1} = F_1 + \mu_D F_1 \mathrm{sgn}(\dot{X}) \tag{9}$$

or

$$F_{T1} = F_1\left[1 + \mu_D \mathrm{sgn}(\dot{X})\right] \tag{10}$$

Using the definition of F_1 from Equation (6), the equation for the total force becomes

$$F_{T1} = k_1 X\left[1 + \mu_D \mathrm{sgn}(\dot{X})\right] \tag{11}$$

Corresponding equations for the draft gear on the struck car are

$$F_{T2} = F_2 + F_{D2} \tag{12}$$

$$X' = X_2 = X_{D2} \tag{13}$$

$$F_2 = k_2 X_2 \tag{14}$$

or $$F_2 = k_2 X' \tag{15}$$

and $$F_{T2} = k_2 X'\left[1 + \mu_D \operatorname{sgn}(\dot{X}')\right] \tag{16}$$

where

F_{T2} = the total force applied to the draft gear on the struck car [lb (force)]

F_2 = the force causing displacement of the spring in the struck car draft gear [lb (force)]

F_{D2} = the force causing displacement of the damper in the struck car draft gear [lb (force)]

X' = the total displacement or travel of the draft gear on the struck car (in.)

X_2 = the displacement of the spring in the struck car draft gear (in.)

and X_{D2} = the displacement of the damper in the struck car draft gear (in.)

The coupler subsystem of Figure 2(a) can now be reduced to the equivalent arrangement shown in Figure 2(b). The total forces acting on the draft gears may now be expressed in terms of the spring constants of the equivalent springs

$$F_{T1} = k_{RCDG} X \tag{17}$$

and $$F_{T2} = k_{FDG} X' \tag{18}$$

where

$$k_{RCDG} = k_1\left[1 + \mu_D \mathrm{sgn}(\dot{X})\right] \tag{19}$$

and

$$k_{FDG} = k_2\left[1 + \mu_D \mathrm{sgn}(\dot{X}')\right] \tag{20}$$

For two springs in series, the total force applied is the same as that on each spring,

$$F_T = F_{T1} = F_{T2} \tag{21}$$

and the total relative displacement or travel of the two springs is equal to the sum of the relative displacements of each of the springs,

$$X_T = X + X' \tag{22}$$

For a single equivalent spring, the total force may be defined as

$$F_T = k_T X_T \tag{23}$$

where

X_T = the total relative displacement of a single spring representing both draft gears (in.)

and k_T = the spring constant of the single equivalent spring [lb (force)/in.]

Solving Equations (17), (18) and (23) for the displacements and substituting into Equation (22) gives

$$\frac{F_T}{k_T} = \frac{F_{T1}}{k_{RCDG}} + \frac{F_{T2}}{k_{FDG}} \tag{24}$$

but since Equation (21) is true, Equation (24) may be reduced to

$$\frac{1}{k_T} = \frac{1}{k_{RCDG}} + \frac{1}{k_{FDG}} \tag{25}$$

or

$$k_T = \frac{k_{RCDG}k_{FDG}}{k_{RCDG} + k_{FDG}} \tag{26}$$

Before this definition of k_T can be used for the submodel of Figure 2(c), both k_{RCDG} and k_{FDG} must be expressed in terms of $\dot{X}_T$ rather than as functions of $\dot{X}$ and $\dot{X}'$. The total travel of the combined draft gears may be expressed as

$$X_T = X_{RC} - X_F \tag{27}$$

and the velocity as

$$\dot{X}_T = \dot{X}_{RC} - \dot{X}_F \tag{28}$$

Combining Equations (17) and (23) gives the relationship between X and X_T,

$$X = \frac{k_T}{k_{RCDG}} X_T \tag{29}$$

and combining Equations (18) and (23) gives the corresponding relationship between X' and X_T,

$$X' = \frac{k_T}{k_{FDG}} X_T \tag{30}$$

Differentiating Equations (29) and (30) with respect to time gives

$$\dot{X} = \frac{k_T}{k_{RCDG}} \dot{X}_T \tag{31}$$

and

$$\dot{X}' = \frac{k_T}{k_{FDG}} \dot{X}_T \tag{32}$$

Substituting from Equations (31) and (32) into Equations (19) and (20) makes both k_{RCDG} and k_{FDG} functions of $\dot{X}_T$,

$$k_{RCDG} = k_1 \left[1 + \mu_D \mathrm{sgn}\left(\frac{k_T \dot{X}_T}{k_{RCDG}}\right)\right] \tag{33}$$

$$k_{FDG} = k_2 \left[1 + \mu_D \mathrm{sgn}\left(\frac{k_T \dot{X}_T}{k_{FDG}}\right)\right] \tag{34}$$

but, since only the sign and not the magnitude of $\dot{X}_T$ is of interest and since k_T, k_{RCDG} and k_{FDG} are always positive,

$$k_{RCDG} = k_1 \left[1 + \mu_D \mathrm{sgn}(\dot{X}_T)\right] \tag{35}$$

and

$$k_{FDG} = k_2 \left[1 + \mu_D \mathrm{sgn}(\dot{X}_T)\right] \tag{36}$$

Equations (35) and (36) define the equivalent spring constants of the draft gears in their "active" state, i.e., when the total displacement lies between its upper and lower limits. When these limits are reached, the draft gears go "solid", i.e., they behave like a solid beam with properties consistent with the structural characteristics of the draft gears and rail cars. Consequently, the definitions of k_{RCDG} and k_{FDG} must be modified to represent the transition from the "active" to "solid" states. This is accomplished by branching within the submodel equivalent to the following:

$$\left.\begin{aligned} k_{RCDG} &= k_1 \left[1 + \mu_D \mathrm{sgn}(\dot{X}_T)\right] \\ k_{FDG} &= k_2 \left[1 + \mu_D \mathrm{sgn}(\dot{X}_T)\right] \end{aligned}\right\} \quad X_{TL} < X_T < X_{TU} \tag{37}$$

and

$$\left.\begin{aligned} k_{RCDG} &= k_{SDG1} \\ k_{FDG} &= k_{SDG2} \end{aligned}\right\} \qquad X_T \le X_{TL} \text{ or } X_T \ge X_{TU} \tag{38}$$

where

X_{TL}, X_{TU} = the lower and upper limits, respectively, on the travel of the combined draft gears (in.)

k_{SDG1}, k_{SDG2} = the spring constants of the "solid" draft gears on the hammer car and struck cars, respectively [lb (force)/in.]

In the submodel, this branching is accomplished by the use of switching functions. In Fortran notation,

```
KRCDG=RSW(XT.LT.XTU.AND.XT.GT.XTL,K1*(1.+MUD*SGNF(DXT)),KSDG1)   (39)
```

and

```
KFDG=RSW(XT.LT.XTU.AND.XT.GT.XTL,K2*(1.+MUD*SGNF(DXT)),KSDG2)   (40)
```

where

RSW ( ) = a "real switch" function in ACSL (Advanced Continuous Simulation Language)

and SGNF ( ) = a specially constructed "signum function".

As a simple general example of how the real switch function works in ACSL, let

R = RSW (A,B,C).

If A is TRUE R = B ,
Otherwise R = C .

The foregoing has been a presentation of the development of the coupler subsystem submodel. The same general approach will be applied to the suspension subsystem submodel since a Barber stabilized truck[1] utilizes friction damping where friction is proportional to the load.

The coupler submodel described here was used to simulate an actual impact between two loaded 70 ton cars at approximately 6 miles/hour. The calculated results are presented in Figures 3 and 4 as coupler force as a function of time during impact. Results from the impact test, as reported by Baillie,[2] are also presented in Figures 3 and 4 for comparison.

The results obtained from the model agree reasonably well with the actual results for the periods when the draft gears are "active", but deviate considerably for the period when the draft gears have gone "solid" after bottoming out. Roggeveen[3] simulated the same test using an analogue computer and obtained the same general trend of results. He concluded that the lower peak force during the actual test could be attributed to energy dissipation due to lading slip or cargo shift, and developed a model which divided the masses of each car into two masses, one for the car and one for the lading. This "two lump" approach was not pursued to its ultimate outcome in the development of the coupler subsystem submodel discussed here since the immediate objective was to devise a submodel to simulate the hysteresis-type behavior of the draft gears during their "active" state. The complete cask-rail car model described earlier in previous progress reports already includes cargo (cask) and truck movement relative to the rail car. However, a "two-lump" representation of the struck car might be appropriate later.

The hysteresis-type behavior of the combined draft gears during their "active" state is illustrated in Figures 5 and 6 which show coupler force as a function of the travel of the combined gears. As long as X_T increases ($\dot{X}_T > 0$), the combined draft gear follows the upper curve, but when X_T decreases ($\dot{X}_T < 0$) it immediately jumps to the lower curve. This action is made possible by the construction and logic of Equations (37). These equations may be expanded to accommodate a piece-wise linear variation of force with displacmement (i.e., linked spring constants) and different values of μ_D for the compression and expansion strokes in the "active" state, to simulate almost any desired behavior.

Figures 3 and 5 present the results obtained from the model when the spring constants of the "solid" gears, k_{SDG1} and k_{SDG2}, were giver a value of 5 x 10^5 lb (force)/in., and Figures 4 and 6 present the results obtained when this value was increased to 1 x 10^6 lb (force)/in. The lower value of the spring constant for the "solid" draft gear lowers the peak force and increases the duration, while the higher spring constant increases the peak force and decreases the duration. The parameters used in the simulation are summarized in Table 1.

B. DATA COLLECTION AND REDUCTION

1. Preliminary Tests

The testing sequence began in June 1978, with a simulated cask (42.5 ton concrete weight) mounted on the Union Carbide railcar. This test successfully demonstrated the test setup and procedures. Additionally, operating experience was gained prior to the tests involving shipping casks.

The preliminary tests were conducted at 5.5, 7.6 and 11.8 mi/hr. In each case, as during subsequent tests, the railcar under test was accelerated by a locomotive to a specific speed determined by radar. When released this car would coast to impact. The railcar under test (hammer car) impacted the first (anvil car) of a set of four loaded and coupled coal cars with slack removed and brakes set.

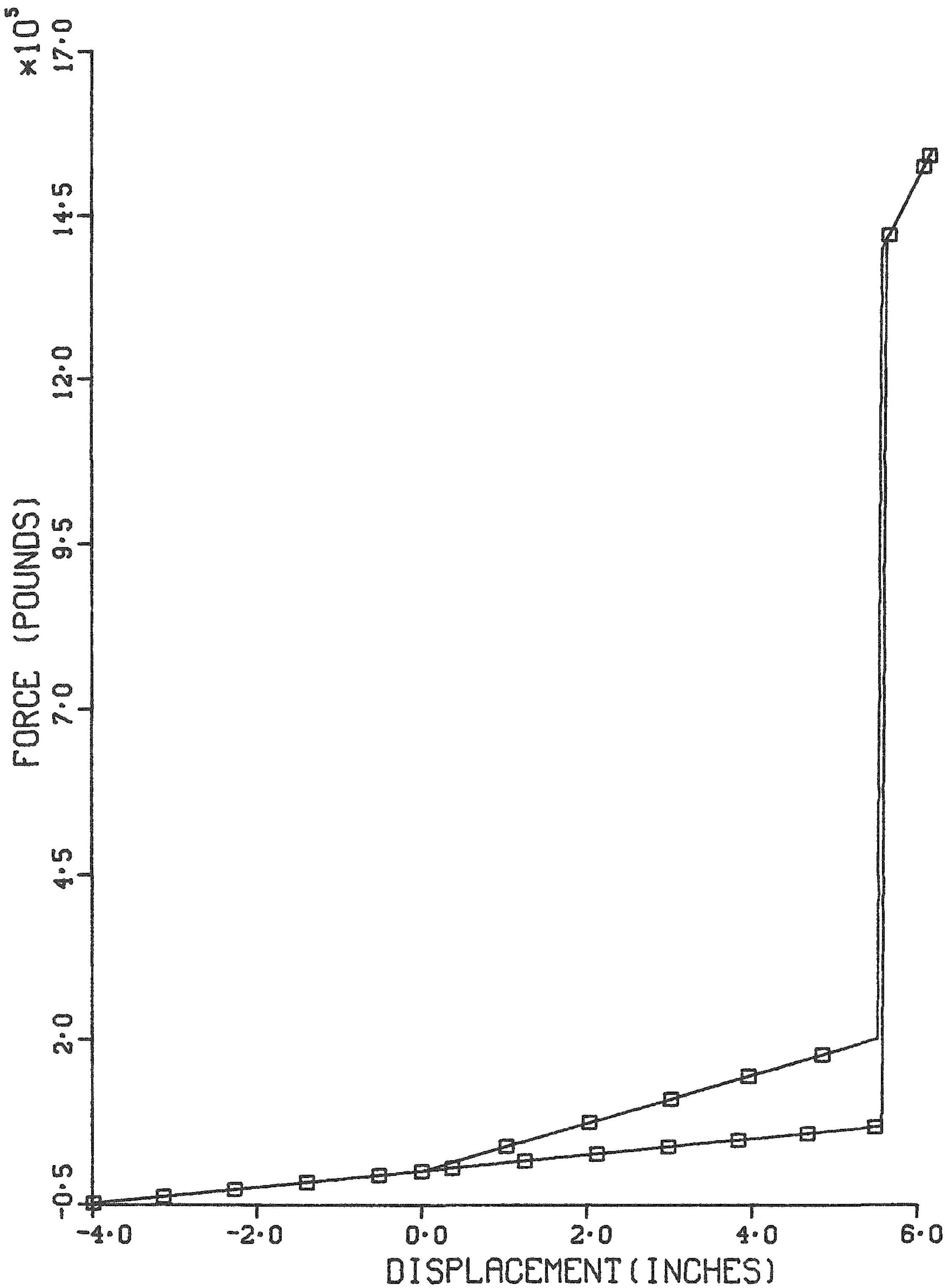

FIGURE 5. Coupler Force vs Displacement of Draft Gears During Impact of Two Loaded Hopper Cars (Spring Constant of "Solid" Draft Gears = 5×10^5 lb/in.).

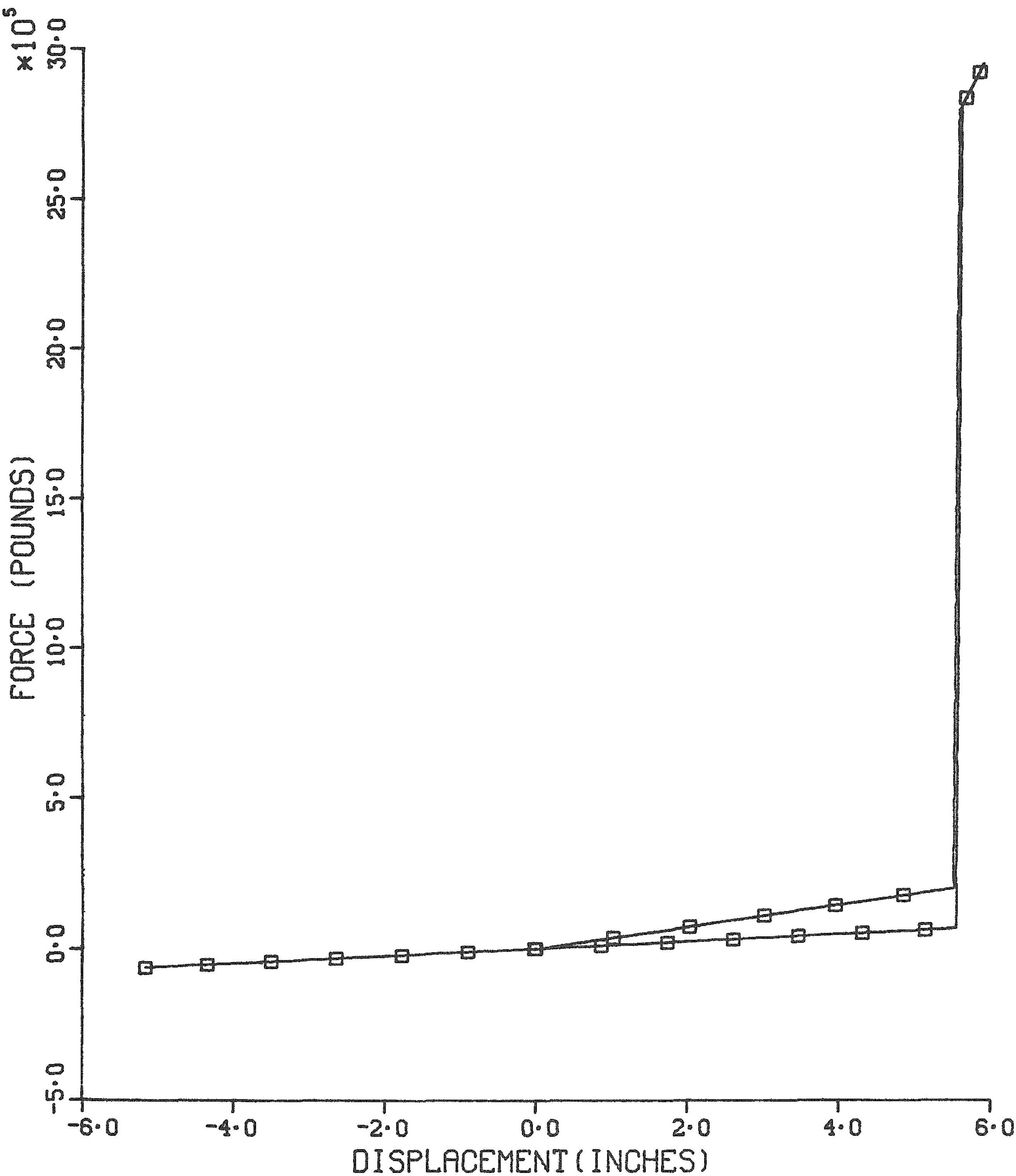

FIGURE 6. Coupler Force vs Displacement of Draft Gears During Impact of Two Loaded Hopper Cars (Spring Constant of "Solid" Draft Gears = 1×10^6 lb/in.).

TABLE 1

PARAMETERS USED FOR SIMULATION OF RAIL CAR
IMPACT TEST BY COUPLER SUBSYSTEM SUBMODEL

Weight of Hammer Car (lb)		
W_{RC}		218,000
Weight of Struck Car (lb)		
W_F		215,000
Spring Constants of Springs in the Draft Gears [lb (force)/in.]		
k_1, k_2		48,666
Pseudo Coefficient of Friction for the Draft Gears		
μ_D		0.5
Velocity of Hammer Car Before Impact (mi/hr)		
V_{XRCI}		5.83
Velocity of Struck Car Before Impact (mi/hr)		
V_{XFI}		0
Limits of Draft Gear Travel (in.)		
X_{TU} (upper)		5.6
X_{TL} (lower)		-5.6
Spring Constants of "Solid" Draft Gears [lb (force)/in.]		
k_{SDG1}, k_{SDG2}	Case 1	5×10^5
k_{SDG1}, k_{SDG2}	Case 2	1×10^6

The only instrumentation during these preliminary tests was high speed photographic coverage. Visual inspection by railraod representatives, following each test, confirmed that no structural damage occurred.

2. Tie-down Tests

Shipping cask tie-down testing with instrumentation designed to monitor shock and vibration was initiated in July 1978. Eighteen railcar impact tests were completed in August 1978 and resulting data are presently being reduced and analyzed. The objective of these tests is to produce data to verify the analytical models of the railcars and the shipping container tie-down systems during impact.

Various configurations of shipping casks, cask tie-down systems, railcar couplers and impact speeds were instrumented and tested as shown in Table 2. The variables in these tests include:

Railcars:
- 80 ton Union Carbide (Paducah) converted for military use -- Figure 7
- 70 ton Seaboard Coastline Railroad (SCL) -- Figure 8

Coupler:
- Standard
- Freight Master end-of-car (EOC) cushioning
- Sliding Sill cushioning

Shipping Cask:
- 42.5 ton concrete simulation
- 40 ton Hallam Cask -- Figure 7
- 70 ton Cask -- Figure 8

Tie-Down System:
- Bolted with stop
- Cable with stop
- Cable without stop

Stop Frequency (f_n): - High frequency -- Figure 9
- Lower frequency -- Figure 10

Speed: - 2 to 11 mi/hr

3. Data Acquisition

Instrumentation configurations were developed to be compatible with the railcar-cask tie-down system being tested. The instruments, together with the mechanical configuration they support, are illustrated in Figures 9 through 12. A brief description of this instrumentation is given in Table 3. The data acquisition techniques previously described[4] were employed.

As during the "preliminary tests", high speed photogrametric instrumentation recorded the coupling action of the railcar under test, as well as the interactions of the railcar, shipping cask, and the tie-down mechanism. Additionally, still photographic records were made of the instrumentation, railcar, shipping cask, and tie-down assembly (Figures 7 and 8).

During these impact tests, the velocity of the railcar under test was accurately measured just prior to impact. The technique employed was to break glass wands with a protrusion extending from the moving railcar. Since the wands were of known separation, the elapsed time between the rods allowed accurate velocity measurements. These values agreed with those from radar measurements.

4. Data Reduction

The photogrametric instrumentation (high speed movies) has been edited and transcribed onto a video tape. An annotated version is nearly complete. The original Sandia FM-FM instrumentation tapes were transcribed to the wide-band FM format required at HEDL (Hanford Engineering Development Laboratory). Data reduction is underway.

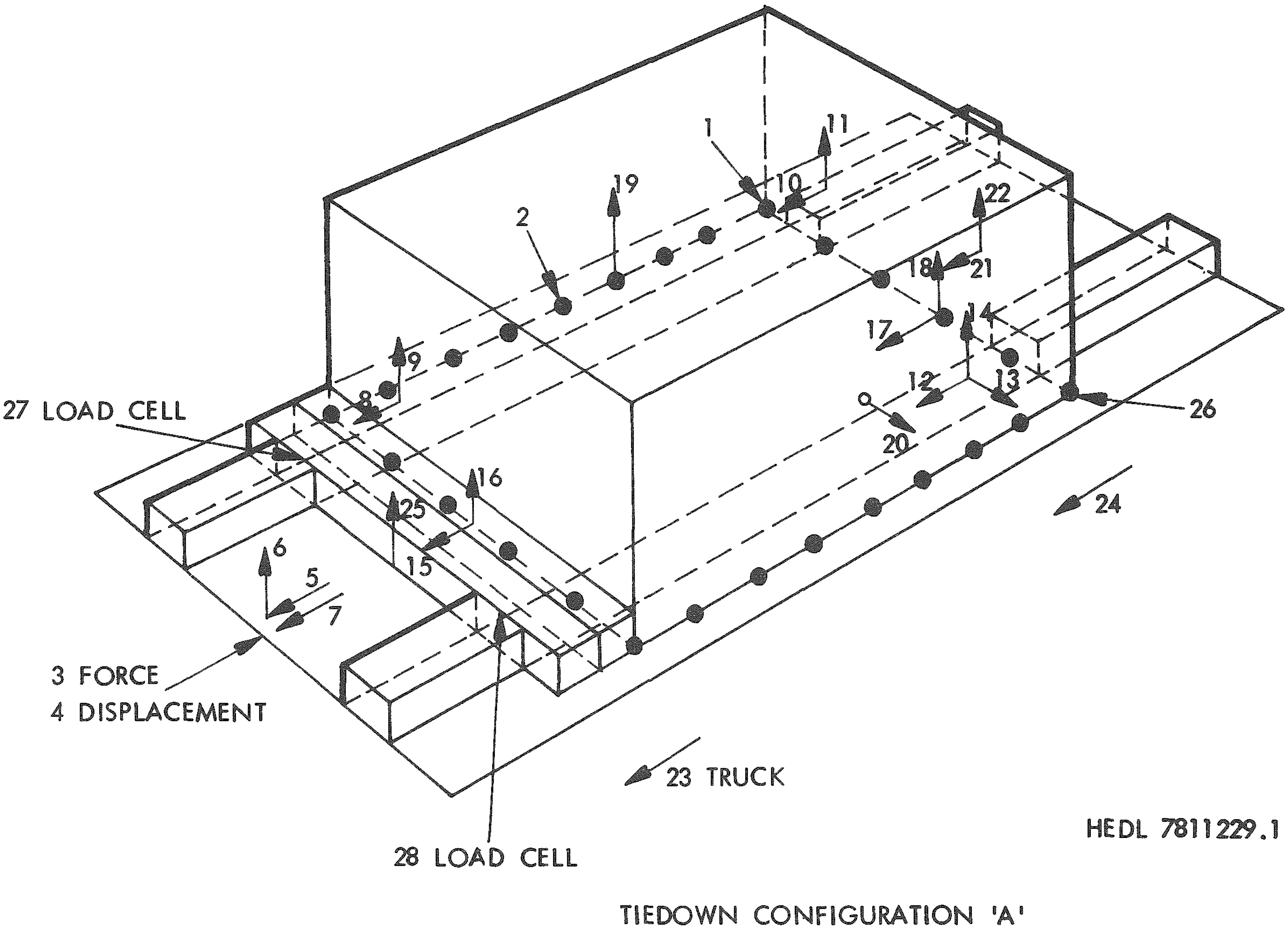

FIGURE 9. Tiedown Configuration and Instrument Location for Cask-Rail Car-Tiedown Tests (Tiedown Configuration "A").

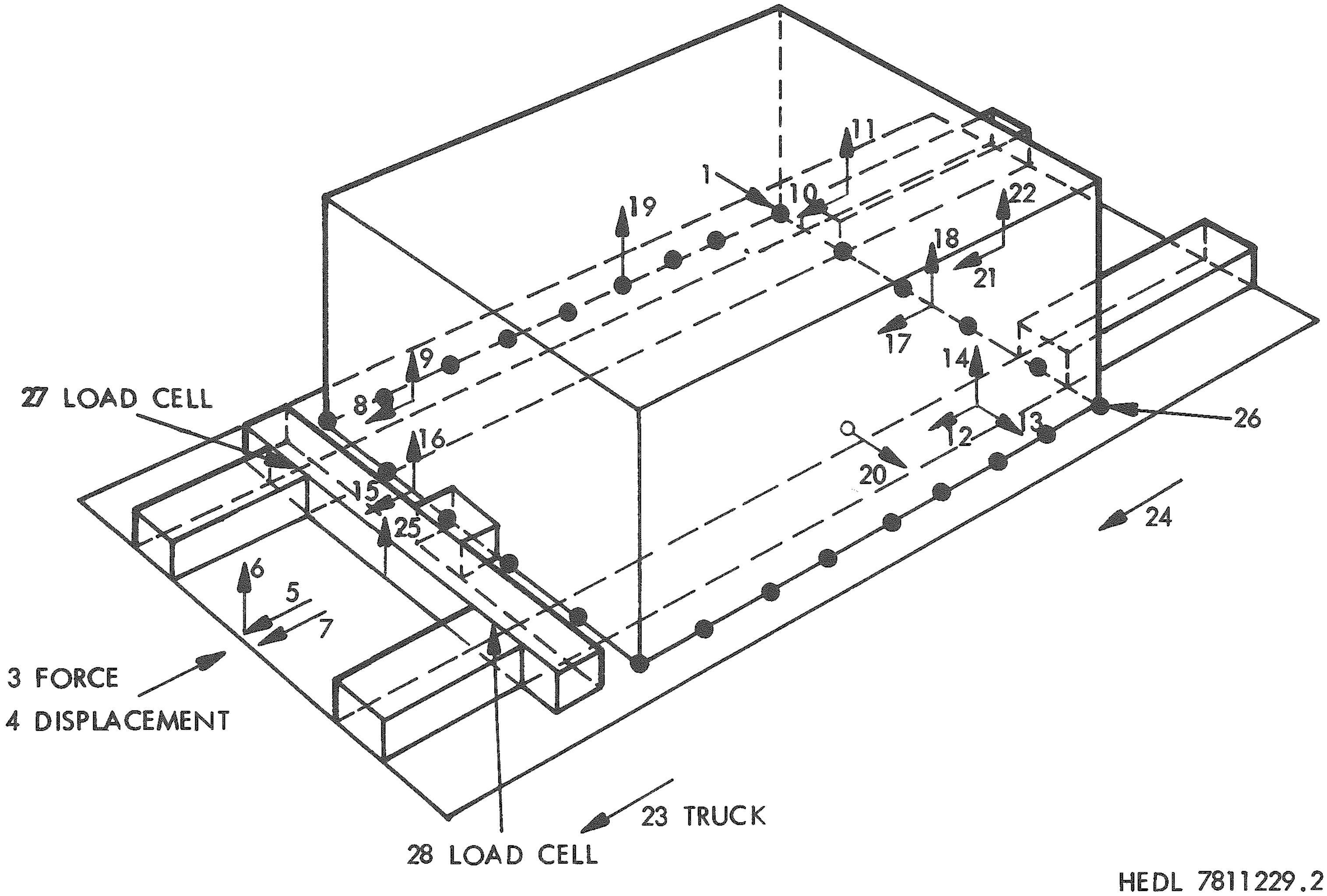

TIEDOWN CONFIGURATION 'B'

FIGURE 10. Tiedown Configuration and Instrument Location for Cask-Rail Car-Tiedown Tests (Tiedown Configuration "B").

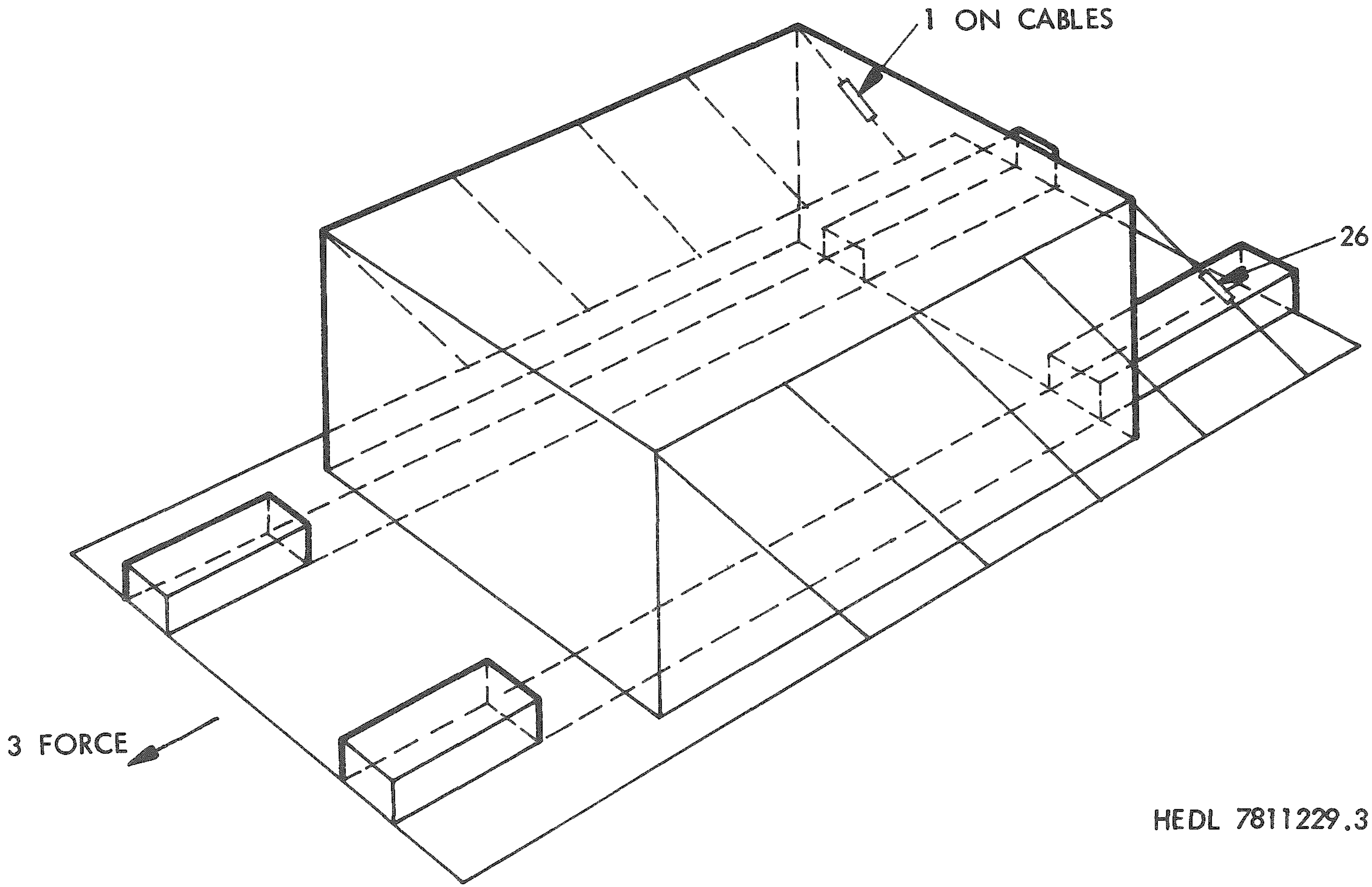

TIEDOWN CONFIGURATION 'C'

FIGURE 11. Tiedown Configuration and Instrument Location for Cask-Rail Car-Tiedown Tests (Tiedown Configuration "C").

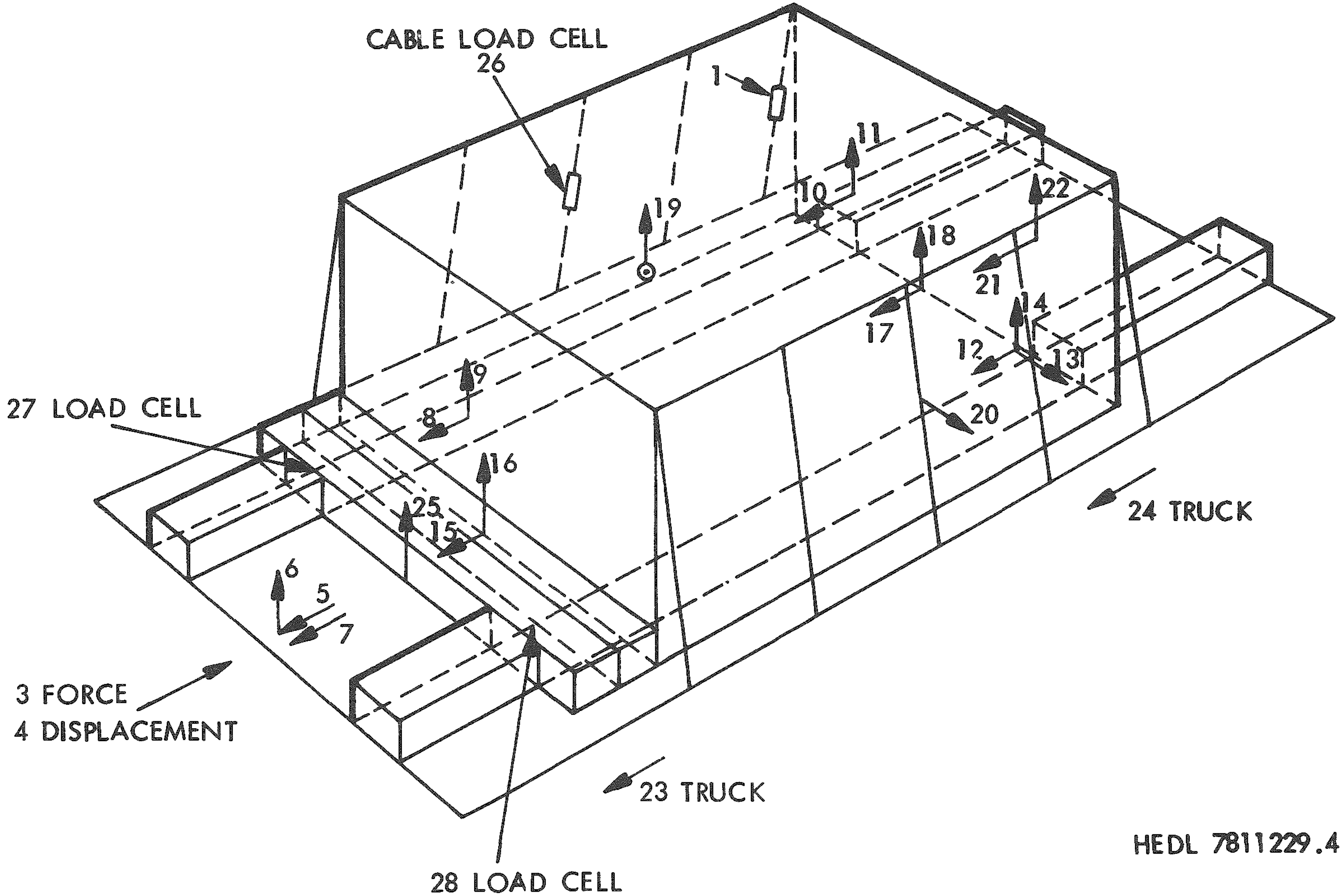

TIEDOWN CONFIGURATION 'D'

FIGURE 12. Tiedown Configuration and Instrument Location for Cask-Rail Car-Tiedown Tests (Tiedown Configuration "D").

TABLE 3

INSTRUMENT CONFIGURATION FOR CASK-RAIL CAR-TIEDOWN TESTS

CONFIGURATIONS A AND B

Instrument No.	Instrument Location	Instrument Type	Measurements
1	Bolt Holddown (FE)*	Instrumented Bolt	Change in Tension
2	Bolt Holddown (Side)	Instrumented Bolt	Change in Tension
3	Coupler	Bridge Type	Force/Time
4	Struck End Of Car	Displacement	Displacement/Time
5	Car Structure (SE)*	PR Accelerator	Shock
6	Car Structure (SE)	PR Accelerator	
7	Car Structure (SE)	PE Accelerator	
8	Cask (SE)	PR Accelerator	
9	Cask (SE)	PR Accelerator	
10	Cask (FE)	PR Accelerator	
11	Cask (FE)	PR Accelerator	
12	Car/Cask Interface	PR Accelerator	
13	Car/Cask Interface	PR Accelerator	
14	Car/Cask Interface	PR Accelerator	
15	Cask Base (SE)	PE Accelerator	
16	Cask Base (SE)	PE Accelerator	
17	Cask Base (FE)	PE Accelerator	
18	Cask Base (FE)	PE Accelerator	
19	Cask Top Center	PE Accelerator	
20	Cask Side Center	PE Accelerator	
21	Car Structure (FE)	PE Accelerator	Shock
22	Car Structure (FE)	PE Accelerator	Shock
23	Truck (SE)	PE Accelerator	Shock
24	Truck (FE)	PE Accelerator	Shock
25	Rail Car Above Truck Center (SE)	PE Accelerator	Shock
26	Bolted Holddown (FE)	Instrument Bolt	Change in Tension
27	Base/Chock Interface (SE)	Load Cell	Change in Compression
28	Base/Chock Interface (SE)	Load Cell	Change in Compression

*SE = STRUCK END
FE = FAR END

TABLE 3 (Cont'd)

INSTRUMENT CONFIGURATION FOR CASK-RAIL CAR-TIEDOWN TESTS

CONFIGURATIONS C** AND D

Instrument No.	Instrument Location	Instrument Type	Measurements
1	Cable (FE)*	Load Cell	Change in Tension
2			
3	Coupler	Bridge Type	Force/Time
4	Struck End Of Car	Displacement	Displacement/Time
5	Car Structure (SE)*	PR Accelerator	Shock
6	Car Structure (SE)	PR Accelerator	
7	Car Structure (SE)	PE Accelerator	
8	Cask (SE)	PR Accelerator	
9	Cask (SE)	PR Accelerator	
10	Cask (FE)	PR Accelerator	
11	Cask (FE)	PR Accelerator	
12	Car/Cask Interface	PR Accelerator	
13	Car/Cask Interface	PR Accelerator	
14	Car/Cask Interface	PE Accelerator	
15	Cask Base. (SE)	PE Accelerator	
16	Cask Base (SE)	PE Accelerator	
17	Cask Base (FE)	PE Accelerator	
18	Cask Base (FE)	PE Accelerator	
19	Cask Top Center	PE Accelerator	
20	Cask Side Center	PE Accelerator	
21	Car Structure (FE)	PE Accelerator	
22	Rail Car Above Truck Center (FE)	PE Accelerator	Shock
23	Truck (SE)	PE Accelerator	Shock
24	Truck (FE)	PE Accelerator	Shock
25	Rail Car Above Truck Center (SE)	PE Accelerator	Shock
26	Cable (FE)	Load Cell	Change in Tension
27	Base/Chock Interface (SE)	Load Cell	Change in Compression
28	Base/Chock Interface (SE)	Load Cell	Change in Compression

*SE = STRUCK END **Only Instrument No's 1, 3 and 26 on Configuration C.

FE = FAR END

As expected, some data acquisition channels failed during tests, similarly, some estimated peak amplitudes (used during calibration of the systems) were too large or too small producing either data which was on the same order of magnitude as the background noise or was clipped off at the saturation level of the system. Although these problems voided the data on the affected channels, these losses should not affect the model validation objective.

The significance of lost data will not be finalized until data reduction has been completed.

C. VALIDATE MODEL

Validation of the cask-rail car dynamic model will be deferred until completion of Task 1 (Develop Dynamic Model) and Task 2 (Data Collection and Reduction).

D. COLLECT PARAMETER DATA

The collection of data on key parameters for the cask-rail car dynamic model was resumed during this reporting period. Data were obtained from segments of the railway equipment industry and from a literature search. Numerous books, papers and other documents have been acquired which contain not only parameter data but also information on construction features of rail car components such as draft gears, suspension systems, etc.

A modest data base is being established to supply the needs of the parametric and sensitivity analysis (Task 5). This data base is being structured for use with a simple manual information retrieval technique to allow rapid and thorough access to the particular data types needed, without the expense of a computerized data base management system. However, since this simple retrieval system is based on techniques similar to those used in a computerized system, it may be computerized later if desired.

Ranges of the various data will be established as more information is gathered. The objective will be to establish accepted or median values, with upper and lower bounds.

The collection and processing of parameter and other data will be a continuing effort.

E. PARAMETRIC AND SENSITIVITY ANALYSIS

This task is not scheduled to begin until December 1, 1978.

F. INTERIM REPORT

This report was originally scheduled for preparation on August 1, 1978, however, it was agreed that it will now be considered as a category of reports to document significant, completed accomplishments prior to completion of the final report (Task 7).

G. FINAL REPORT

This report is not scheduled for preparation until August 1, 1979.

IV. REFERENCES

1. C. L. Combes, et al, 1966 Car and Locomotive Cyclopedia, 1st Edition, Simmons-Boardman Publishing Corporation, NY, NY, 1966.

2. W. E. Baillie, "Impact as Related to Freight Car and Lading Damage", ASME Paper 59-A-249.

3. R. C. Roggeveen, "Analog Computer Simulations of End Impact of Railway Cars," ASME Paper 65-RR-3.

4. S. R. Fields and S. J. Mech, Dynamic Analysis to Establish Normal Shock and Vibration Environments Experienced by Radioactive Material Shipping Packages, Quarterly Progress Report January 1, 1978 - March 31, 1978, NUREG/CR-0161, (HEDL-TME 78-41), Hanford Engineering Development Laboratory, Richland, WA, July 1978.

NUREG/CR-0589
HEDL-TME 78-102
RT

DISTRIBUTION

DOE/Richland Operations (5)
P. O. Box 550
Richland, WA 99352

Manager
Chief Patent Attorney
B. J. Melton
J. D. White (2)

DOE/FFTF Project Office
P. O. Box 550
Richland, WA 99352

Director

DOE Chicago Patent Group
9500 S. East Avenue
Argonne, IL 60439

A. A. Churm

DOE Environmental Control and Technology Division
Washington, DC 20545

J. Counts

Hanford Engineering Development Laboratory (35)
P. O. Box 1970
Richland, WA 99352

G. L. Mack W/C-123 (35)

Pacific Northwest Laboratory
P. O. Box 999
Richland, WA 99352

L. D. Williams

E. I. DuPont de Nemours and Company
P. O. Box A
Aiken, SC 29801

S. F. Petry

Los Alamos Scientific Laboratory
P. O. Box 1663
Los Alamos, NM 87545

T. D. Butler

Sandia Laboratories
P.O. Box 5800
Albuquerque, NM 87115

C. F. Magnuson